Talanta 80 (2009) 246–249

Contents lists available at ScienceDirect

Talanta

journal homepage: www.elsevier.com/locate/talanta

Fabrication of a novel impedance cell sensor based on the polystyrene/polyaniline/Au nanocomposite

Miaomiao Gu, Jingjing Zhang, Ye Li, Liping Jiang, Jun-Jie Zhu*

Key Lab of Analytical Chemistry for Life Science (MOE), School of Chemistry and Chemical Engineering, Nanjing University, 22 Hankou Road, Nanjing 210093, PR China

ARTICLE INFO

Article history:
Received 3 March 2009
Received in revised form 26 June 2009
Accepted 28 June 2009
Available online 4 July 2009

Keywords:
Gold nanoparticles
PS@PANI
HL-60 cells
Biosensor
Electrochemical impedance spectroscopy

ABSTRACT

Gold nanoparticles (AuNPs) were assembled on the surface of polystyrene (PS) and polyaniline (PANI) core–shell nanocomposite (PS@PANI) for the immobilization of HL-60 leukemia cells to fabricate a cell electrochemical sensor. The immobilized cells exhibited irreversible voltammetric response and increased the electron transfer resistance with a good correlation to the logarithmic value of concentration ranging from 1.6×10^3 to 1.6×10^8 cells mL^{-1} with a limit of detection of 7.3×10^2 cells mL^{-1} at 10σ. This biosensor was simple, low cost and disposable, which implied that the PS@PANI/Au composites can regard as the potential applications for clinical applications.

1. Introduction

In recent years, there is an increasing demand to use rapid and simple procedures for the detection of cells viability and proliferation. A series of important biochemical and physiological processes in a living cell involve electron generation and transfer. Therefore, the electrochemical and photoelectric techniques have attractive considerable attention for studying efficiently intact living cells [1,2]. For example, the voltammetric responses of the redox centers in living cells usually show irreversible electron transfer processes [3]. This has been used to characterize the viability of cells in homogeneous solution. However, the anodic peak currents in cyclic voltammograms of cells were generally weak. It is important for searching some methods to improve the electrochemical response signal.

With unique chemical and physical properties, gold nanoparticles (AuNPs) are nowadays the subject of a wide field of research [4,5]. Particularly, there is an enormous interest in exploiting gold colloids in biotechnology for biosensing, imaging, and drug delivery [6,7]. Incorporation of AuNPs with polymers or inorganic materials has attracted increasing interest in improving the stability and biocompatibility to enhance the capability of immobilization. Among these materials, polyaniline (PANI) has been proven particularly useful in the development of biosensors, because of its low cost, readily film forming ability, chemical and electrochemical stability [8]. Polystyrene (PS) latex beads are a kind of functional polymer materials, which have many admirable properties such as biocompatibility, nontoxicity, high surface area and chemical inertness. Taking into account the advantages of PS, PANI and AuNPs, the core–shell nanocomposite has been fabricated, and was applied to assemble a glucose biosensor [9]. As far as I know, it was not used for the detection of cells concentration and monitoring the growing states of tumor cells.

Electrochemical impedance spectroscopy (EIS) is usually regarded as an effective way for probing the interfacial properties and has been used to develop the cell sensors [10–12]. Herein, gold nanoparticles were combined with core–shell nanocomposite (PS@PANI) to form a novel 3D architecture conjunction (PS/PANI/Au), which can be further used to immobilize HL-60 leukemia cells to fabricate a cell electrochemical sensor. The biosensor was more effective for the rapid determination of cell concentration ranging from 1.6×10^3 to 1.6×10^8 cells mL^{-1} with a limit of detection of 7.3×10^2 cells mL^{-1} at 10σ. Moreover, the 3D architecture interface can be used for the electrochemical monitoring of the cells adhesion and proliferation, leading a rapid, simple, and more importantly, convenient way to study and monitor the viability of living tumor cell.

2. Experimental

2.1. Materials

Aniline, styrene, ammonium persulfate ($(NH_4)_2S_2O_8$, APS), potassium persulfate ($K_2S_2O_8$, KPS), $HAuC1_4$ and trisodium cit-

* Corresponding author. Tel.: +86 25 83594976; fax: +86 25 83594976.
E-mail address: jjzhu@nju.edu.cn (J.-J. Zhu).

0039-9140/$ – see front matter © 2009 Elsevier B.V. All rights reserved.
doi:10.1016/j.talanta.2009.06.065

rate ($C_6H_5O_7Na_3{\cdot}2H_2O$) were purchased from Shanghai Chemical Reagent Company. Aniline and styrene were distilled under reduced pressure before use. Poly(sodium 4-styrenesulfonate) (PSS, M_w ~70,000) was from Aldrich Chemical Company. Phosphate buffer solution (PBS) (pH 7.4) containing NaCl 137 mM, KCl 2.7 mM, $Na_2HPO_4{\cdot}12H_2O$ 87.2 mM, and KH_2PO_4 14.1 mM was used as electrolyte. All other reagents were of analytical grade and used without further purification.

2.2. The preparation of the core–shell PS/PANI/Au nanocomposite interface

The glass carbon electrode (GCE) was first polished with 1.0, 0.3, and 0.05 μm alumina slurry successively, and then rinsed with doubly distilled water. The PS/PANI/Au nanocomposite was prepared according to the literature [9]. The obtained nanocomposite was then dispread in water to form a 5.0 mg mL^{-1} solution by sonication. Finally, 5 μL of PS/PANI/Au sol was dropped onto the GCE to form a nanocomposite film (PS/PANI/Au/GCE). The modified electrode was stored in air prior to use.

2.3. Cells culture and immobilization

HL-60 cells were cultured in a flask in RPMI 1640 medium (GIBCO) supplemented with 10% fetal calf serum (FCS, Sigma), penicillin (100 μg mL^{-1}), and streptomycin (100 μg mL^{-1}) at 37 °C in a humidified atmosphere containing 5% CO_2. At the growth retardation stage 3 days, the cells reached a number of 1.0×10^7 cell mL^{-1}, which was determined using a Petroff–Hausser counter (USA). They were collected and separated from the medium by centrifugation at 1000 × *g* for 10 min, followed by washing twice with a sterile PBS (pH 7.4) and resuspending in PBS to obtain cell suspension. Finally, 5 μL of the cell suspension was dropped on the PS/PANI/Au modified GCE, and was incubated at 37 °C for 2 h to achieve cell immobilization.

2.4. Apparatus

The morphologies of the PS/PANI/Au nanocomposite were characterized by scanning electron microscopy (SEM, LEO1530VP) and transmission electron microscopy (TEM, JEOLJEM-200CX).

Cyclic voltammetric and amperometric experiments were conducted with a CHI660B workstation (Shanghai Chenhua, Shanghai).

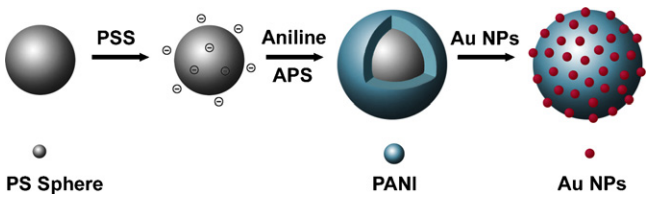

Scheme 1. Schematic illustration of the synthesis of complex PS/PANI/Au.

All experiments were carried out using a conventional three-electrode system in 0.1 M PBS, where nanocomposite-modified GCE was used as working electrode, a platinum wire as auxiliary electrode and a saturated calomel electrode (SCE) as reference electrode. EIS measurements were carried out on a PGSTAT30/FRA2 system (Autolab, Netherlands) using the three-electrode system in solution containing 10 mM $Fe(CN)_6^{3-/4-}$ and 1.0 M KCl. The impedance spectra were recorded within the frequency range of 10^{-2} to 10^6 Hz. The amplitude of the applied sine wave potential in each case was 5 mV. The applied DC potential was about 0.18 V.

3. Results and discussion

3.1. Characterization of the PS/PANI/Au nanocomposite

The formation of the three-component nanocomposite was described in Scheme 1. Briefly, PSS was modified onto the surface of PS beads for the purpose of increasing the negative charges. Then the positive charged aniline monomer was adsorbed onto the PSS modified PS beads. Through in situ polymerization, PS/PANI core–shell structural composite could be obtained. The Au-decorated PS/PANI nanocomposite was finally formed by an electrostatic effect after introducing PS/PANI into the negative charged Au colloid. Fig. 1 shows the typical TEM and SEM images of the PS/PANI/Au nanocomposite. The PS/PANI/Au nanocomposite with an average diameter of 500 nm was uniform in size and morphology. The numerous individual dark nanodots spread along the grey nanospheres in Fig. 1A and the corresponding outside particles in Fig. 1B are AuNPs, which indicates that well-dispersed AuNPs decorate the core–shell structured PS/PANI surface quite uniformly. The nanoparticle-decorated core–shell nanocomposite can be used to fabricate a cell-based biosensor due to the excellent conductivity of PANI and prominent biocompatibility of AuNPs. The biocom-

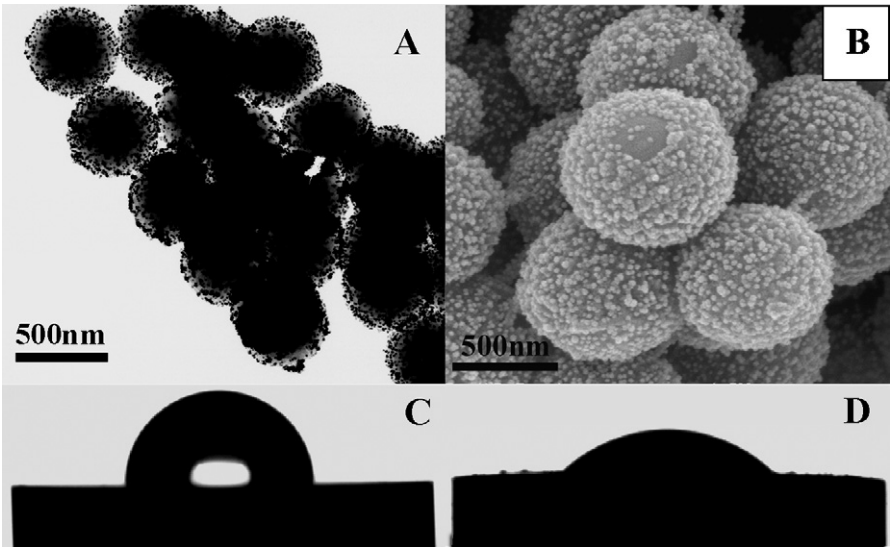

Fig. 1. (A) TEM and (B) SEM images of the PS/PANI/Au nanocomposite. Contact angle of bare electrode (C) and PS/PANI/Au modified electrode (D).

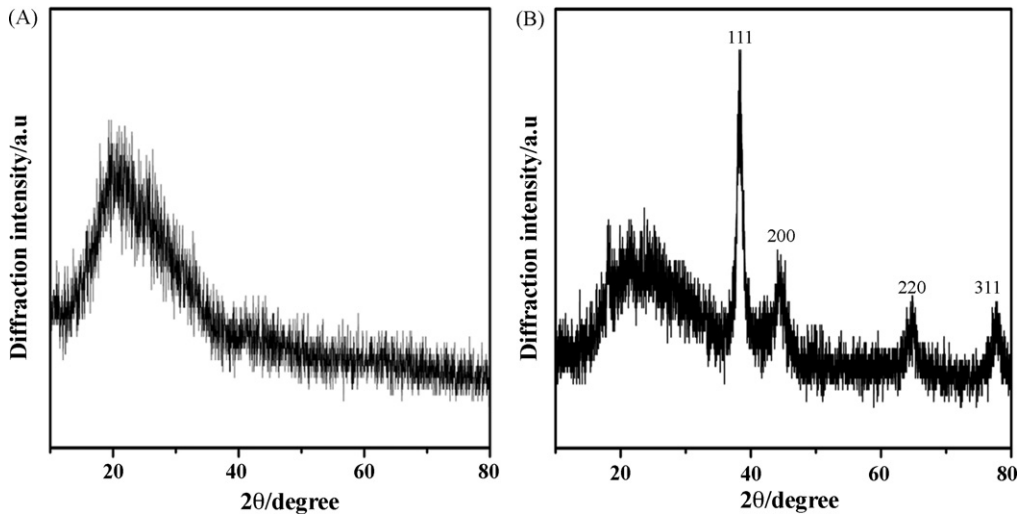

Fig. 2. The XRD patterns of the PS/PANI nanocomposite (A) and the PS/PANI/Au nanocomposite (B).

patibility for loading biomolecules and preserving their bioactivity could be characterized by the hydrophilicity, which could be measured by the contact angle of the substrate. As shown in Fig. 1 (C and D), the contact angle of the bare and PS/PANI/Au modified electrode surface was of 92° (C) and 46° (D) respectively, which indicates the high hydrophilicity of PS/PANI/Au. Thus, the prepared nanocomposite could offer a high hydrophilic surface for promoting cell adhesion and retaining cell activity.

In order to prove Au NPs have been attached on the PS/PANI nanospheres, XRD measurement was carried out. Fig. 2A shows the XRD pattern of the PS/PANI nanospheres, and there was only a broad peak at 22°, which can be assigned to the periodicity parallel to the polymer chains of PANI. While in Fig. 2B, which indicates the XRD pattern of PS/PANI/Au nanocomposite, four additional peaks located at about 38°, 44°, 65°, and 77° are observed besides the broad peak located at 22°. Those peaks can be assigned to the (1 1 1), (2 0 0), (2 2 0), and (3 1 1) lattice planes of fcc-Au.

3.2. Cyclic voltammetric behavior of HL-60 cells on modified electrode

It is well known that many important processes in living cells possess certain electrochemical characteristics. Electron generation and charge transfer exist in all living cells due to the redox reactions and the changes of ionic composition and concentration in life processes [13]. Fig. 3 shows the electrochemical behavior of living cells immobilized on PS/PANI/Au modified electrode. Owning to the larger accessible surface area of the modified electrode, the background current of the PS/PANI/Au modified GCE (Fig. 3b) was greater than that of bare GCE (Fig. 3a). At the modified GCE, the HL-60 tumor cell suspension showed a well-defined irreversible oxidation peak at +0.87 V, while no peak was observed on both bare and PS/PANI/Au (Fig. 3c) modified GCE. The irreversible oxidation peak disappeared in the second scan, and no corresponding reduction peak appeared in the inverse scan, which is the characteristic of an irreversible electrode process. The conversion of guanine in cell cytoplasm to 8-oxo-guanine led to the irreversible electrochemical response of HL-60 tumor cells. In the electrochemical process, the guanine molecules could go through the cell membrane rapidly [14]. Considering the irreversibility of the electrode process of HL-60 cells, the peak current on the first scan was applicable to study tumor cells viability.

3.3. Impedance characteristics of modified electrodes

The electrochemical impedance spectra (EIS) of the modified electrodes were shown in Fig. 4. The electron transfer resistance (R_{et}) was extracted parameters by fitting the EIS data into a suitable equivalent circuit on each independently fabricated electrode. The R_{et} can be used to describe the interface properties of the electrode [15]. At a bare GCE, the redox process of the probe showed a low electron transfer resistance 41.2 Ω (Fig. 3a). When PS/PANI/Au

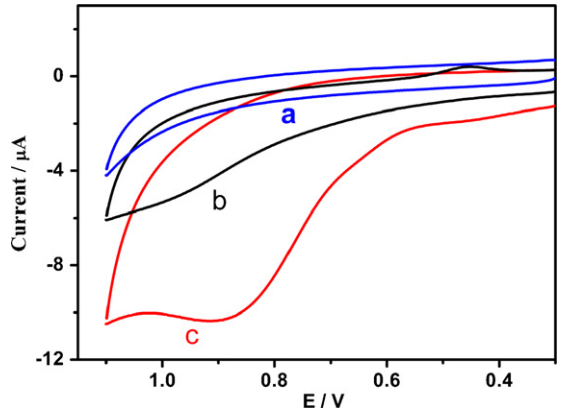

Fig. 3. Cyclic voltammograms of bare GCE (a), PS/PANI/Au/GCE (b), and cells/PS/PANI/Au/GCE (c) in pH 7.4 PBS. Scan rate: 50 mV s^{-1}.

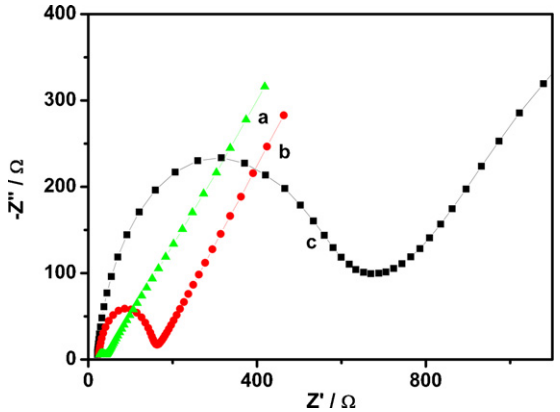

Fig. 4. Nyquist diagrams of electrochemical impedance spectra of bare GCE (a), PS/PANI/Au/GCE (b), and cells/PS/PANI/Au/GCE (c).

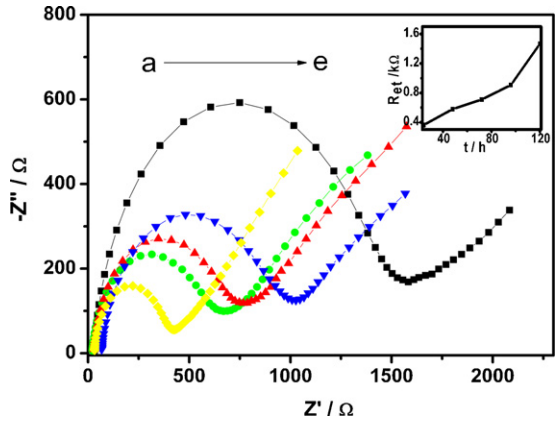

Fig. 5. EIS measurements of HL-60 cells proliferated on PS/PANI/Au/GCE after cell incubation for (a) 24 h, (b) 48 h, (c) 72 h, (d) 96 h and (e) 120 h. Inset: relationship between electron transfer resistance and proliferation time of HL-60 cells on PS/PANI/Au/GCE.

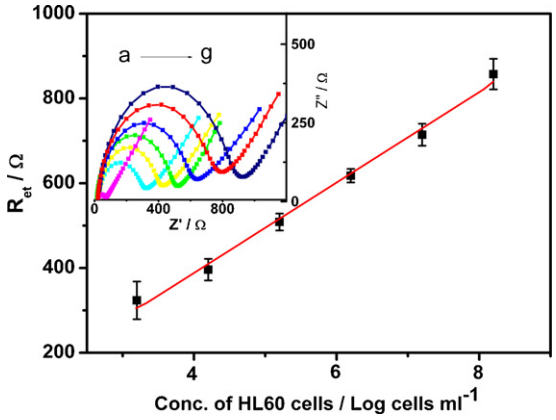

Fig. 6. Linear relationship between electron transfer resistance and logarithm of HL-60 cells concentration. Inset: Nyquist diagrams of PS/PANI/Au modified GCE after immersed in (a) 0 cells mL^{-1}, (b) 1.6×10^3 cells mL^{-1}, (c) 1.6×10^4 cells mL^{-1}, (d) 1.6×10^5 cells mL^{-1}, (e) 1.6×10^6 cells mL^{-1}, (f) 1.6×10^7 cells mL^{-1}, and (g) 1.6×10^8 cells mL^{-1} HL-60 cells suspension.

was assembled on the bare electrode, the semicircle increased dramatically (Fig. 3b). The R_{et} value was about 133.3 Ω, suggesting that the assembly of the nanocomposite layer on the electrode surface inhibited the interfacial electron transfer. When cells were attached to the PS/PANI/Au/GCE, a barrier of the cell membrane would further hinder the redox probe close to the electrode surface and increase the R_{et} value to 601.0 Ω (Fig. 3c). The increasing impedance depended on the surface coverage of the cells, which was proportional to the concentration of the cells used in the adhesion process.

3.4. Monitoring of cell proliferation on electrode surface

EIS measurement was further used to monitor the change of support surface resulting from cell proliferation. Electrochemically monitoring of cell proliferation could be achieved conveniently by placing a set of cells/PS/PANI/Au in culture medium in batch, and measuring at different incubation times. As seen from Fig. 5, with the increasing incubation time, the electron transfer resistance of the redox probe at the produced electrode increased (curves a–e). Obviously resulted from the cell proliferation on the electrode, the increasing amount of cells could lead to a greater barrier for electrochemical process. The inset in Fig. 5 indicates that the R_{et} increased gradually up to the incubation time of 48 h and then tended to a relatively steady value during the incubation time of 48–96 h. After 96 h a sharply increasing resistance was observed, indicating that a majority of HL-60 cells was already dead. This change might be related to the apoptosis of cells, which was congregated on the electrode surface.

3.5. Impedance detection of HL-60 cells

The PS/PANI/Au/GCE could be used for the detection of HL-60 cell concentration. With the increasing concentration of HL-60 cells, the R_{et} value increased, showing increasing diameter of the semicircle on the Nyquist diagram (inset of Fig. 6), implying a higher amount of HL-60 cells immobilized on the electrode. The R_{et} value was proportional to the logarithm of HL-60 cells concentration ranging from 1.6×10^3 to 1.6×10^8 cells mL^{-1} (Fig. 6), with a correlation coefficient of 0.9965. The limit of detection was calculated to be 7.3×10^2 cells mL^{-1} at 10σ, which was comparable with those of several methods developed by other researchers such as the impedance immunosensor for *Escherichia coli* O157:H7 [11] and EIS technique for leukemia K562 cells [16]. Five different biosensors were tested independently for the detection of cells concentration, providing the RSD value of 2.47%.

4. Conclusions

While fabricating a sensitive impedance cell sensor, we took the advantageous features of PANI and gold nanoparticle to construct a nontoxic biocompatible interface for immobilization of tumor cells. Gold nanoparticles with excellent biocompatibility was used to modify leukemia HL-60 cells, which could not only efficiently preserve the activity of tumor cells, but also accelerate the electron transfer between electrode and the immobilized cells. The cell-based impedance sensor showed the wide detection range, low detection limit, good detection precision and simple fabrication process, which could be further developed as a convenient means for the study of cells adhesion, proliferation and apoptosis.

Acknowledgments

The work was supported by the National Natural Science Foundation of China for the Key Program (20635020), Creative Research Group (20821063), and National Basic Research Program of China (2006CB933201).

References

[1] Y.X. Ci, C.Y. Zhang, J. Feng, Bioelectrochem. Bioenerg. 45 (1998) 247.
[2] C. Hao, F. Yan, L. Ding, Y.D. Xue, H.X. Ju, Electrochem. Commun. 9 (2007) 1359.
[3] J. Feng, G.A. Luo, H.Y. Jiang, R.G. Wang, C.C. An, Electroanalysis 12 (2000) 513.
[4] M.C. Daniel, D. Astruc, Chem. Rev. 104 (2004) 293.
[5] H. Vallhov, J. Qin, S.M. Johansson, N. Ahlborg, M.A. Muhammed, A. Scheynius, S. Gabrielsson, Nano Lett. 6 (2006) 1682.
[6] F. He, Q. Shen, H. Jiang, J. Zhou, J. Cheng, D.D. Guo, Q.N. Li, X.M. Wang, D.G. Fu, B.A. Chen, Talanta 77 (2009) 1009.
[7] J.J. Li, L. Zou, D. Hartono, C.N. Ong, B.H. Bay, L.Y. Lanry Yung, Adv. Mater. 20 (2008) 138.
[8] A. Morrin, F. Wilbeer, O. Ngamna, S.E. Moulton, A.J. Killard, G.G. Wallace, M.R. Smyth, Electrochem. Commun. 7 (2005) 317.
[9] Y.G. Liu, X.M. Feng, J.M. Shen, J.J. Zhu, W.H. Hou, J. Phys. Chem. B 112 (2008) 9237.
[10] C.Z. Li, Y. Liu, J.H.T. Luong, Anal. Chem. 77 (2005) 478.
[11] L. Yang, Y. Li, G.F. Erf, Anal. Chem. 76 (2004) 1107.
[12] C. Ruan, L. Yang, Y. Li, Anal. Chem. 74 (2002) 4814.
[13] W. Nonner, B. Eisenberg, J. Mol. Liq. 87 (2000) 149.
[14] M.L. Pedano, G.A. Rivas, Electrochem. Commun. 6 (2004) 10.
[15] S. Hleli, C. Martelet, A. Abdelghani, F. Bessueille, A. Errachid, J. Samitier, H.C.W. Hays, P.A. Millner, N. Burais, N. Jaffrezic Renault, Mater. Sci. Eng. C 26 (2006) 322.
[16] H.L. Hu, H. Jiang, X.M. Wang, B.A. Chen, Electrochem. Commun. 10 (2008) 1121.